International Journal of Recent Technology and Applied Science
p-ISSN: 2721-2017, e-ISSN: 2721-7280

Original Research Paper

Impregnation Effect of Synthesized Fe3O4 Nanoparticles on the Jabon Wood's Physical Properties

Istie Rahayu[1*], Rohmat Ismail[2], Wayan Darmawan[1], Irma Wahyuningtyas[3], Esti Prihatini[1], Gilang Dwi Laksono[1], Dhiya Khairunissa[4]

[1] *Department of Forest Products, Faculty of Forestry and Environment, IPB University. Indonesia.*
[2] *Department of Chemistry, Faculty of Mathematics and Natural Sciences, IPB University. Indonesia.*
[3] *Department of Forest Products Processing Technology, Faculty of Environment and Forestry, Samarinda State Agricultural Polytechnic. Indonesia.*
[4] *Department of Chemistry, Faculty of Mathematics and Natural Sciences, Nusa Bangsa University. Indonesia.*

Article History
Received:
29.05.2024

Revised:
30.06.2024

Accepted:
02.07.2024

***Corresponding Author:**
Istie Rahayu
Email:
istiesr@apps.ipb.ac.id

Abstract: This research focused on characterizing synthetic magnetite (Fe3O4-NP) and evaluating the impregnated jabon wood's physical properties. The co-precipitation method used for the synthesis of Fe3O4-NP, namely by mixing the iron solution (n/n Fe2+:Fe3+=1:2) with the strong base of sodium hydroxide (NaOH) (MG-S) and weak base of ammonium hydroxide (NH4OH) (MG-W) as precursors. The impregnation stage uses parameters of a -0.5 bar vacuum for half an hour and 2 bar pressure for 2 hours with magnetite concentrations of 1; 2.5; 5% w/v in a demineralized water solvent. Scanning electron microscopy-energy dispersive x-ray spectroscopy (SEM-EDX) and Fourier transform infrared spectrometry (FTIR) confirmed the presence of Ferrum content and Fe-O functional group in both Fe3O4-NPs produced. The Fe3O4-NP size was also measured via the X-ray diffraction analysis, namely 34.54 nm for the MG-S and 39.24 nm for the MG-W. Magnetic strength obtained was 7.51 mT for the MG-S and 8.58 mT for the MG-W. The impregnated jabon wood's physical properties also improved with indications of an increase in wood density, weight percent gain (WPG), bulking effect (BE), anti-swelling efficiency (ASE), and a decrease in water absorption (WA). The results showed the best treatments were MG-S 2.5% and MG-W 5%.

Keywords: *Anthocephalus cadamba*, Fe3O4, Impregnation, Nanoparticles, Physical Properties.

1. Introduction

Currently, metal nanoparticles have quite a lot of attention from many researchers since their uniqueness, making them have a lot of potential applications in various sectors. They can be utilized in biology, pharmacy, textiles and food industries, biology, and so forth [1]. This is because nanoparticles exhibit high stability, an even particle size distribution, and a relatively high surface-to-volume ratio [2]. Because of their small size, they can permeate deep within the wood's hollow spaces, preventing them from damage caused by solar radiation and biological warfare [3]. Several metal nanoparticles that abundant in the industry, including silver (Ag), gold (Au), copper (CuO), titanium dioxide (TiO_2), iron oxide (Fe_2O_3), magnetite (Fe_3O_4), and many more [4]. In this study, magnetite nanoparticles (Fe_3O_4-NP) were employed to enhance the quality of fast-growing wood.

Typically, Fe_3O_4-NP has an inverse spinel structure that includes oxygen and iron atoms in a tight cubic package, with the positions being tetrahedral and octahedral. This particular structure allows Fe_3O_4-NP to become a ferromagnetic and semi-conductive material [5]. Fe_3O_4-NP can be prepared by adding ammonium hydroxide (NH_4OH) and sodium hydroxide (NaOH) as base precursors to the iron mixture solutions during the synthesis process in addition to generating the small and homogeny sizes in both kinds of Fe_3O_4-NP [6]. This method is also known as the co-precipitation method. Then, the wood modification was introduced, precisely wood impregnation, which makes it possible for Fe_3O_4-NP to incorporate in the wood cavities. Earlier studies [7], [8] conducted the fast-growing wood impregnation using Fe_3O_4-NP and successfully invented a new promising material called magnetic wood.

Through the impregnation process of Fe_3O_4-NP, jabon wood (*Anthocephalus cadamba* Miq.) is expected to have excellent basic properties and expand its uses, which makes the attractiveness of jabon wood increase. As known, jabon wood has low physical and mechanical properties because of its juvenile wood content [9]. This condition is unfavorable for wood users because of its short useful life, thus wood impregnation is necessary. It can also overcome the community's need for wood considering the wood availability from natural forests is dwindling. This impregnated wood also has good magnetic properties, so it can be used as the material of medical tools, furniture, building construction, and radar wave absorbers emitted from electronic instruments [10], [11]. Thereby, this study is to characterize the two types of Fe_3O_4-NP, resulting from the co-precipitation method, and compare the impregnation effects on the jabon wood's physical properties.

2. Literature Review

2.1. Wood Chemistry

The chemical components of wood consist of structural and extractive components. The structural components are insoluble macromolecules that are responsible for forming the cell wall structure and maintaining the cell configuration thus supporting most of the wood properties either physically or chemically. These structural components can be declined from the cell wall by the depolymerization process with the application of chemical or mechanical treatment. Through this process, the wood's characteristics and cellular properties are transformed substantially. Therefore, cellulose, hemicellulose, and lignin are categorized as wood structural components. On the other hand, extractive components are unstructured components found in wood's cell lumina, cellular cavities or channels. These organic components can be extracted from wood by using solvents with sufficient polarity, without changing their cellular structural characteristics. Extractive components mostly contain various chemical compounds that in general have a low molecular mass and only some are in polymeric form. The inorganic component is part of the extractive component and is usually only a small part (<1%) often referred to as wood ash [12].

2.2. Jabon Wood

Jabon wood (*Anthocephalus cadamba*) is a fast-growing wood originating from South Asia and Southeast Asia, one of which is Indonesia and has a wood texture that is slightly fine to slightly rough, straight fibrous, less shiny and odorless [13]. Jabon wood is a light wood with lots of usage, among others: raw materials for plywood, lightweight construction, flooring, pulp and paper, ceilings, boxes, crates, toys, carvings, matches, chopsticks and pencils. Jabon wood has a specific gravity of about 0.42 (0.29-0.56), including Strength Class III-IV, Durability Class V, almost entirely radially multiple diffuse pores consisting of 2-3 pores with a diameter of 130-220 μm, and a frequency of 2-5

per mm^2 with simple perforation planes [14]. According to research conducted by [15], jabon wood has a fresh moisture content of 118.43% and an air-dried moisture content of 15.36%.

2.3. Wood Modification

Wood modification is a term for converting the properties of wood materials, which encompasses all processes of applying chemical, mechanical, physical or biological methods. Wood modification involves the action of chemical, biological or physical agents on the material to produce an improvement in its properties and quality. Wood modification can involve active modification, which results in a change in the chemical properties of the material, or passive modification, where there is a change in characteristics without changing the chemistry. Wood impregnation modification is another type of modification. This method is the impregnation of the wood cell wall with a chemical or combination of chemicals to form a material that is "locked" to the cell wall. Wood impregnation is a passive modification process, which means that although the properties of the wood are affected, there is no change in its chemistry [16].

2.4. Magnetite

Magnetite (Fe_3O_4) is a type of iron oxide mineral that naturally occurs on Earth. This material has a cubic crystal system which is described by the general formula $Fe^{2+}Fe^{3+}{}_2O_4$ (Fe_3O_4). Magnetite can be easily found in the environment because it is contained in anthropogenic materials (e.g. coal fly ash) resulting from human activity and synthetic products (e.g. black toner powder). Various geological commodities generally contain this material in the natural phase, ranging from igneous rocks (e.g. layered ultrabasic rocks, basalts) to sedimentary (e.g. beach sand) rocks, and high-grade metamorphic rocks. Furthermore, magnetite formation occurs through chemical reactions and can be used as a reactive substance to investigate the oxygen levels in rocks throughout the geological processes and changes in atmospheric oxygen content [17].

3. Methodology

3.1. Materials

This study used a random sampling method to gain a 5-year-old defect-free jabon wood with a 25-28 cm diameter (*Anthocephalus cadamba* Miq.) which was felled from people's forest in Bogor, West Java. The chemicals used in the study included $FeCl_3.6H_2O$ (Merck), $FeCl_2.4H_2O$ (Merck), ethylenediaminetetraacetic acid (EDTA) (Merck), sodium hydroxide (NaOH) (Merck), ammonium hydroxide (NH_4OH) (Merck), hydrochloric acid (HCl) (Merck), universal pH indicator paper (Merck), and demineralized water.

3.2. Method

- **The Procurement of Wood Sample**

Jabon wood was cut without considering the portion of sapwood and heartwood, according to British Standard [18] (2 × 2 × 2) cm^3. A total of 40 wood pieces were utilized to investigate the effect of Fe_3O_4-NP on jabon wood's physical properties. 10 replications are needed for each concentration to obtain the optimum result.

- **Magnetite-NP Synthesis**

In the present work, we chose the co-precipitation method to produce Fe_3O_4-NP by utilizing both strong and weak base precursors. Iron solutions (the mole ratio of Fe^{2+}/Fe^{3+} = ½) were mixed with chloride hydrate salts in an alkaline medium, and prepared in two different closed Erlenmeyer glasses. To stop the oxidation reaction between Fe^{2+} and to avoid the precipitation of the Fe^{3+} in a hydroxide form, we added 10 mL of each 1 M EDTA and 1 M HCl into both glasses. Then, 125 mL of 0.30 M Fe^{3+} and 0.15 M Fe^{2+} were mixed and stirred for three minutes. It continued by gradually adding 1.5 M base precursors, either NH_4OH or NaOH, in each mixture of iron solution under constant stirring, til their pH reached 12 and a black residue appeared. The black residue was washed with demineralized water until pH 9 and then separated using a magnet and 24 hours oven-dried at 40 °C [19]. The chemical equations below illustrate this synthesis reaction (Eq. 1) [20]:

$$2Fe(OH)_3 + Fe(OH)_2 \rightarrow Fe_3O_4 + 2H_2O \quad (1)$$

- **Wood Impregnation Process**

Firstly, the wood was oven-dried at 103 ± 2 °C until a constant weight was achieved, then its weight and dimension were measured. The solution preparation was performed by an hour homogenizing the synthetic Fe_3O_4-NP and demineralized water using a sonicator CGOLDENWALL 5-200MLLab (300W, Zhejiang, China) with an amplitude of 40%. There were three levels of Fe_3O_4-NP solution used to generate the optimal formulation (Table 1). This process was conducted in three concentrations of Fe_3O_4-NP, namely 1%, 2.5%, and 5% (w/v%) and began by the wood immersion together with the solution in an impregnation tube under a -0.5 bar vacuum for half an hour and a 2 hours pressure of 2 bar. After completion, the wood was polymerized for 12 hours in an oven at 65 °C in aluminum foil-wrapped condition and followed by a drying process at 103 ± 2 °C for 48 hours until the weight remained unchanged, then measured its weight and dimensions.

Table 1. The comparison of the Composition of Fe_3O_4-NP and Demineralized Water

No	Demineralized water (mL)	Fe_3O_4-NP (w/v %)
1	500	1
2	500	2.5
3	500	5

- **Characterization of Magnetite Nanoparticles**

The resulting Fe_3O_4-NP was characterized using several instruments, including a scanning electron microscope (SEM, ZEISS EVO10)-dispersive X-ray spectroscopy (EDX, ZEISS SmartEDX), fourier transform infrared spectrometry (FTIR, Perkin Elmer One Spectrum), x-ray diffraction (XRD, PANalytical Empyrean), UV-Vis Spectrophotometer (Shimadzu 1800), and tesla meter (Simco FMX-003 series TD8620).

- **Physical Properties Evaluation**

The wood's physical properties evaluated in this study were weight percent gain (WPG), anti-swelling efficiency (ASE), water absorption (WA), bulking effect (BE), and density (ρ). The following equations are used to measure the parameters (Eq. 2-6):

$$WPG\ (\%) = \frac{W_1 \quad W_0}{W_0}\ x\ 100 \tag{2}$$

$$ASE\ (\%) = \frac{S_u - S_t}{S_u}\ x\ 100 \tag{3}$$

$$WA\ (\%) = \frac{W_2 - W_1}{W_1}\ x\ 100 \tag{4}$$

$$BE\ (\%) = \frac{V_1 - V_0}{V_0}\ x\ 100 \tag{5}$$

$$\rho\ ((kg/m^3) = \frac{W_1}{V_1} \tag{6}$$

W_0, W_1, and W_2 respectively represent the oven-dried wood mass before and after impregnation, and also the wood mass after 24 hours of water immersion. S_u and S_t are defined as the volume loss of the untreated and impregnated wood. Whereas, V_0 and V_1 are interpreted as the oven-dried wood volume before and after impregnation.

- **Data Analysis**

The data were analyzed using a completely randomized design (CRD) through ANOVA and Duncan's Post Hoc test ($p<0.05$) on the software IBM SPSS Statistics 25 (Statistical Package for Service Solutions) program. Origin 8.5 was also used to elaborate the characterization data.

4. Finding and Discussion

4.1. Characterization of Synthetic Fe_3O_4-NP

The co-precipitation method was chosen in this study because it is easy to work on a laboratory scale with the availability of adequate tools and materials. Moreover, it can also manufacture magnetite products with high yields [21], reaching 93.08% for NaOH precursor and 82.98% for NH_4OH precursor. By utilizing a capping agent like EDTA, it was discovered that this technique could regulate the magnetite nuclei growth, leading to smaller Fe_3O_4-NP size and even-looking morphology [6]. EDTA is hypothesized to have a beneficial effect on the stability and nucleation of Fe_3O_4-NP, which results in nanosized materials with high absorption capacity and surface area [22]–[24]. Furthermore, the synthesized Fe_3O_4-NP was characterized using X-ray Diffraction Spectroscopy (XRD), Fourier Transform Infrared Spectrometry (FTIR), and Tesla meter to confirm that Fe_3O_4-NP impregnated in the jabon wood was identifiable and had good quality characteristics. For details, the properties of the synthesized Fe_3O_4-NP are written in Table 2.

Table 2. Characteristics of synthetic Fe_3O_4-NP

Magnetite Sample	Yield (%)	Magnetic Strength (mT)	Degree of Crystallinity (%)	Crystal Size (nm)
MG-S	93.08	7.51±0.59	86.56	34.54
MG-W	82.98	8.58±0.63	87.25	39.24

MG-S: magnetite synthesized using NaOH precursor
MG-W: magnetite synthesized using NH_4OH precursor

According to the results in Table 2, the MG-S sample exhibits a lower magnetic strength and degree of crystallinity compared to the MG-W sample, but it has a smaller size of nanoparticles. This was thought to be caused by sodium metal residues and its strong alkaline nature. The sodium metal belongs to the diamagnetic and soft metal categories [25], so the magnetic strength and crystallinity may decrease when mixed with Fe_3O_4-NP. However, its high alkalinity led to the rate of formation of Fe_3O_4-NP nuclei becoming higher than the rate of its growth [19], thus producing smaller and more particles which is indicated by the higher yield of the MG-S sample. To support these statements, the diameter of the produced Fe_3O_4-NP can be measured through diffractograms resulting from XRD analysis. The Scherrer equation (Eq. 7) below was used in calculating the crystal size from the diffraction pattern data [26], as shown in Figure 1.

$$D = \frac{K\,\lambda}{\beta \cos\theta} \tag{7}$$

According to this equation, the peak width at a half maximum (FWHM) is defined as a comparison of the diffraction peak broadening (β) to the crystal size (D). The wavelength of the X-ray (0.15418 nm) is denoted by λ. K is the Scherrer constant (0.89), and θ is the Bragg diffraction angle [27]. From the calculation, it can be concluded that the crystal size of formed Fe_3O_4-NP was 34.54 nm and 39.24 nm, sequentially for MG-S and MB-W samples, as written in Table 2. This means the synthetic Fe_3O_4-NPs have been classified as nanoparticles due to their powder size below 100 nm with a crystal size approach [28]. Previous works [19], [29] confirmed that the powder size of Fe_3O_4-NP with a weak base precursor is homogeneously distributed, meanwhile, those using a NaOH precursor exhibited a higher reaction rate at the point of high intensity, thus resulting in smaller particles.

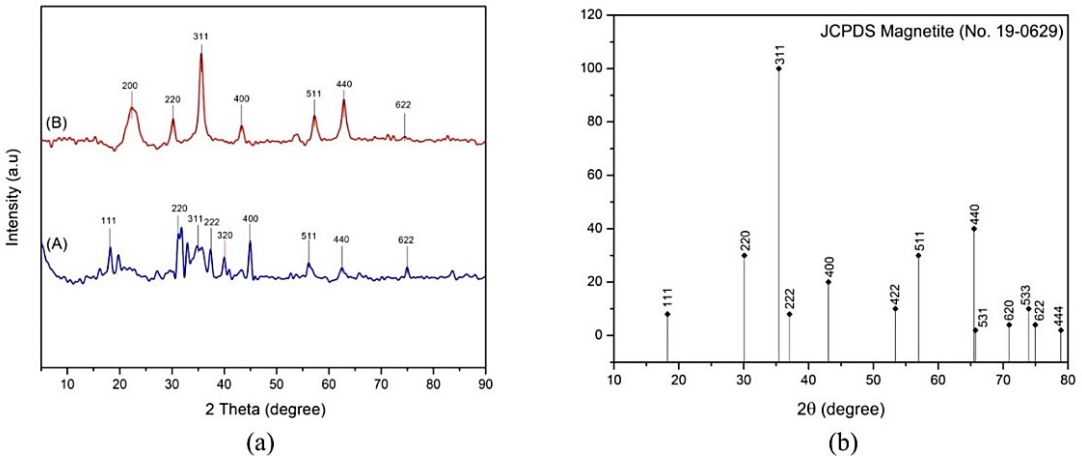

Figure 1. XRD Diffractogram of:
(a) MG-S (A, Blue Line) and MG-W (B, Red Line)
(b) Powder Data File (PDF) Card Magnetite

The crystallite phase of synthetic Fe_3O_4-NP can also be discovered by analyzing the diffraction pattern shown in Figure 1. Several peaks that appeared in the MG-S sample are 2θ = 18.22° (I_{111}), 30.21° (I_{220}), 35.25 (I_{311}), 37.36° (I_{222}), 43.32° (I_{400}), 56.13° (I_{511}), 62.51° (I_{440}), and 74.96° (I_{622}). Similarly, the MG-W sample shows the 2θ which also identifies certain peaks, namely 30.22° (I_{220}), 35.60° (I_{311}), 43.32° (I_{400}), 57.24° (I_{511}), 62.89° (I_{440}), and 74.54° (I_{622}). Analyzed from JCPDS Fe_3O_4 diffractogram No. 19-0629 [30], it can be concluded that these peaks are identified as the peak of Fe_3O_4-NP that a co-precipitation method has been successfully used to synthesize Fe_3O_4-NP. In addition, two peaks of 2θ were also found in the MB-SB and MG-W samples, namely 22.34° (I_{200}) and 39.98° (I_{320}), respectively. These peaks indicate that maghemite (αFe_2O_3) was also formed during the synthesis process, according to the JCPDS Maghemite diffractogram No. 04-0755 [30]. This can be attributed to the fact that magnetite nanoparticles undergo an oxidation reaction with oxygen in the free air, as demonstrated by the chemical equation (Eq. 8) [31]:

$$4Fe_3O_4 + O_2 \rightarrow 6\gamma Fe_2O_3 \rightarrow 6\alpha Fe_2O_3 \quad (8)$$

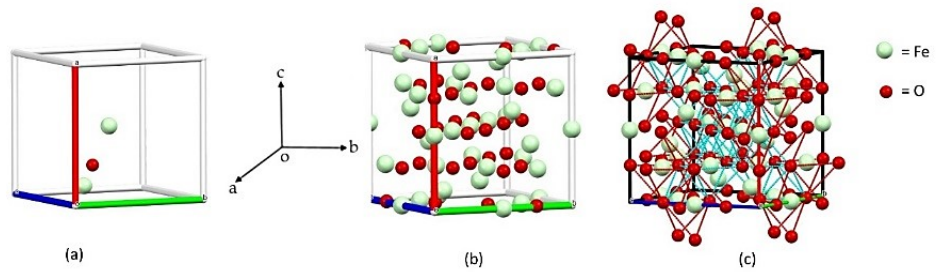

The notations of a, b, c, and o are three-dimensional coordinate systems. An intersection point of the origin (o) is formed by three axes: x (a), y (b), and z (c) which are perpendicular to each other.

Figure 2. The Crystal Structure of Fe_3O_4-NP with a Three-Dimensional Ball and Stick Pattern:
(a) Unit
(b) Atomic Packing
(c) Isometric Shape in a Face-Centered Cubic Crystal Structure

Elucidation of the crystal structure of Fe_3O_4-NP using QualX software and visualized using Mercury software [32]. The crystal structure measurement showed a face-centered cubic crystal shape (Figure 2). The earlier work [33] stated that magnetite crystals have an inverted spinel cubic structure containing Fe ions filling tetrahedral A and octahedral B sites. The ionic structure of Fe_3O_4-NP in the inverted spinel phase is Fe^{3+} (A) $Fe^{2.5+}$ (B) $Fe^{2.5+}$ (B) O_2^{-4}. In addition, magnetite has a space group Fd3m (no. 227) with a lattice constant (a) of about 8.397 Å and the number of atoms per unit cell (Z) is 8 [34].

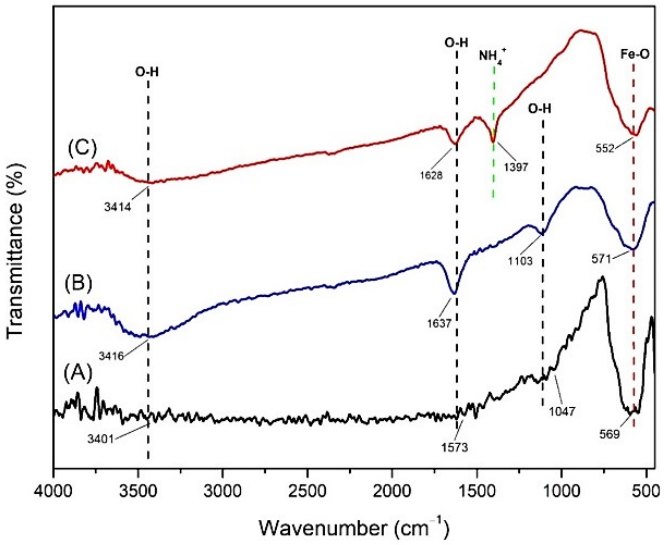

Figure 3. The FTIR Spectrum of:
(a) Commercial Fe_3O_4-NP (Standard)
(b) MG-S
(c) MG-W

In Figure 3, the commercial Fe_3O_4-NP is used as a standard in determining the Fe-O group at a wave number of 569 cm^{-1} which represents the bonded framework of Fe_3O_4. The hydroxyl groups were also detected both in-plane and out-of-plane at wave numbers of 1047, 1573, and 3401 cm^{-1} in the bending vibrations form. This has occurred due to the Fe_3O_4-NP compounds can absorb H_2O on their surfaces [35]. The analytical results of the MG-S and MG-W samples identified all the functional groups similar to the Fe_3O_4-NP standard, especially for the Fe-O functional group with wave numbers of 571 and 552 cm^{-1}. The MG-W sample showed a wave number of 1397 cm^{-1} corresponding to the ammonium ion peak [36]. This peak can be attributed to the ionized residues of NH_4OH during the MG-W synthesis. The O-H functional groups were also found at 3414, 3416, 1628, 1637, and 1103 cm^{-1}. This evidence of the presence of water molecules in the MG-S and MG-W samples was detected. Overall, the analysis results of the MG-S and MG-W samples exhibited the same spectrum pattern after being compared to the FTIR of commercial Fe_3O_4-NP. This indicates that Fe_3O_4-NP was successfully synthesized.

To confirm the Fe_3O_4-NP produced in this study has good magnetic properties, analysis using a Tesla meter was also needed. The magnetic strength results from this instrument will be expressed in units of mili Tesla (mT). From Table 2, it is known that the MG-S sample possesses a magnetic strength of 7.51±0.59 mT, while the MG-W sample is 8.58±0.63 mT. Although the magnetic strength of both samples is not significantly different, this is associated with the degree of crystallinity of the synthetic magnetite. A positive relationship between magnetic properties and the average particle size has been confirmed [37]. The high level of crystallinity and the inert surface layer of the crystal are responsible for the strong magnetic properties [38]. In addition, the supporting data regarding the morphology of Fe_3O_4-NP was also obtained after being investigated under Scanning Electron Microscopy (SEM) in various magnifications (Figure 4).

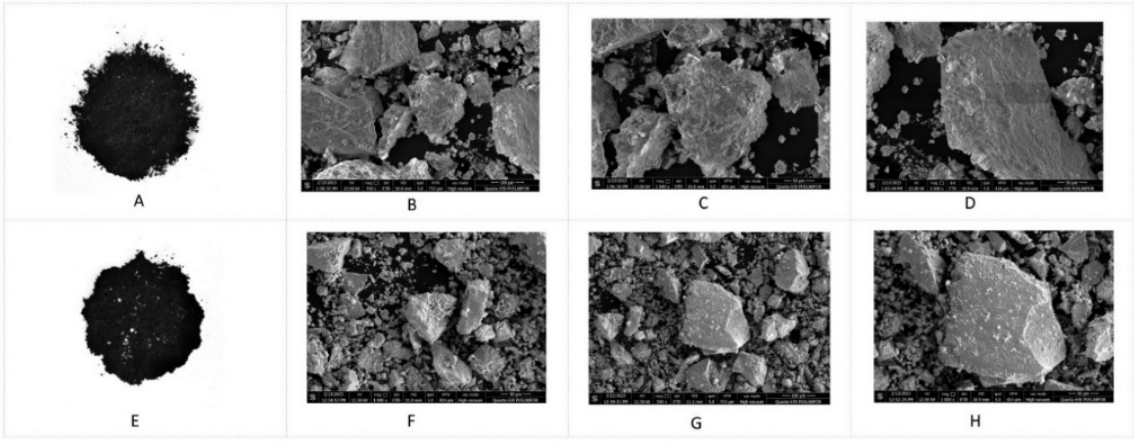

Figure 4. The Morphology of Synthetic Fe_3O_4-NP:
(a) MG-S
(b) 100× MG-S
(c) 250× MG-S
(d) 550× MG-S
(e) MG-W
(f) 100× MG-W
(g) 250× MG-W
(h) 550× MG-W

As predicted, both synthetic Fe_3O_4-NPs show a black color as illustrated by Figures 4a and 4e. This means that Fe_3O_4-NP did not experience an oxidation reaction before the impregnation treatment. Oxidized magnetite will change its color from black to brown due to the presence of rusty particles [39]. Besides, this is because the Fe_3O_4-NP was produced at the optimum chemical condition, thus there was no excess amount of ferrous ions which caused the color to turn brownish. At 100× magnification, both Fe_3O_4-NPs tend to perform spherical particles. It can be seen that MG-W (Figure 4b) generated a smaller and more uniform particle than MG-S (Figure 4f). The increasing magnifications to 250× and 550× make it clear that particle agglomeration cannot be prevented. Fe_3O_4-NP is known to have an attractive dipole force among them that leads to alternating aggregation [40], as shown in Figures 4c-d and Figures 4g-h. In addition, this agglomeration was also related to the role of van der Wall's force [41]. To ensure that Fe_3O_4-NP was formed during the synthesis process, the chemical composition using EDX was also retrieved (Table 3).

Table 3. Chemical Components of Magnetite Nanoparticles

Sample	Fe (wt. %)	O (wt. %)
MG-S	28.9	19.1
MG-W	58.0	23.4

Based on Table 3, the only elements that appeared in this result analysis were Ferrum and oxygen. The Fe elements are more abundant in the MG-W sample which reached 58 wt.%, more than the Fe content in the MG-S sample which only detected as much as 28.9 wt.%. The resulting Fe_3O_4-NP using NH_4OH is evidenced to be homogenous and well distributed compared to the other one, accordingly, it helps deeply penetrate the wood and enhance its physical properties [42]. The lower Fe content in the MG-S sample was suspected by a lot of residue content which is thought originated from sodium metal ions formed during the ongoing Fe_3O_4-NP synthesis process.

To provide complete information, Figure 5 below represents the UV-Vis spectra of both synthetic Fe_3O_4-NPs. The MG-S exhibits a strong wave absorbance at 224.47 nm, whereas the MG-W shows a slightly lower wave absorbance of 222.32 nm. The addition of precursors did not indicate a significant effect in this case. The presence of a coating layer on the Fe_3O_4-NP also causes broadening spectrum peaks or no sharp peaks detected [43]. It is proportionally related to the crystallinity and the maximum absorbance is obtained when the electrons undergo excitation from the valence band to the conduction band [44]. The band gap energy was also measured from the same spectrum (Figure 5) and was clarified by Figure 6. This parameter is calculated using the Tauc method (Eq. 9):

$$(\alpha \cdot hv)^{\gamma} = B\,(hv - E_g) \tag{9}$$

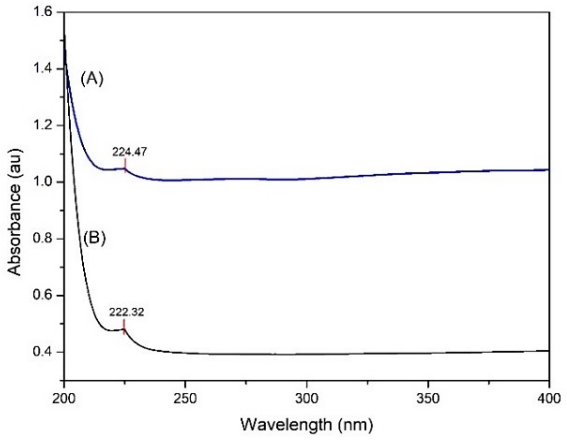

Figure 5. The UV-Vis absorption spectrum of:
(a) MG-S
(b) MG-W samples

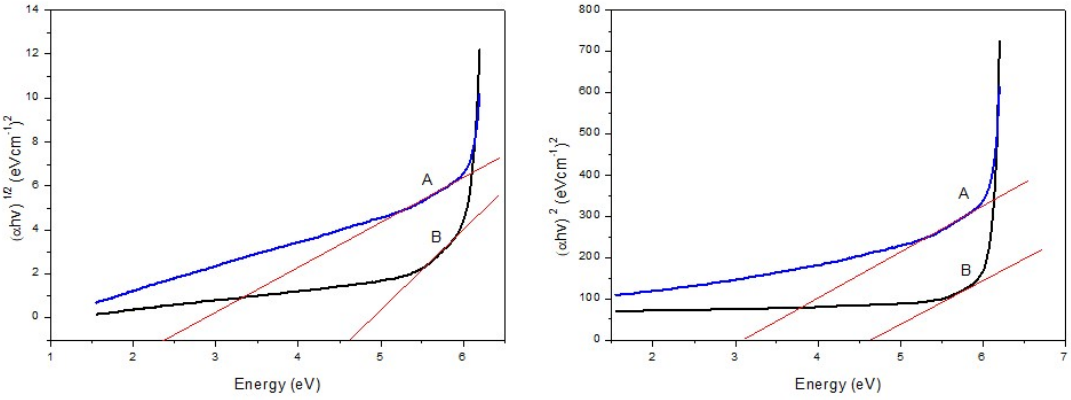

Figure 6. The results of band gap energy analysis of:
(a) MG-S
(b) MG-W samples

Table 4 shows the direct band gap energy released from the MG-S and MG-W samples, namely by up to 1.33 eV and 4.66 eV, consecutively. These results are classified as semiconductor materials. Its narrowband energy produces few electrons in the valence band and rises into the conduction band leaving a hole in the valence band if the temperature increases [45]. Related to the Fe_3O_4-NP size, the

particle energy possible ground state is altered by the addition of lower molecular orbitals, and thus the band gap energy improves with smaller particles [46]. In addition, the indirect band gap energy also shows a linear value, namely 2.33 eV for the MG-S and 4.57 eV for the MG-W samples. Further information can be seen in Table 4.

Table 4. The Band Gap Energy Analysis of Both Fe_3O_4-NPs

Sample	Direct Band Gap Energy (eV)	Indirect Band Gap Energy (eV)
MG-S	3.11	2.33
MG-W	4.66	4.57

4.2. Fe_3O_4-NP Impregnation Effect on Jabon Wood's Physical Properties

Jabon wood exhibited better physical properties after being impregnated with both synthetic Fe_3O_4-NPs. The untreated wood was used as a comparative control, and the outcomes are outlined in Table 5. MG-S 2.5% shows the highest WPG even though it is slightly different from the untreated wood. Due to the residual nature of NaOH, the water solubility of Fe_3O_4-NP can be improved through the hydrogen bonds formation by residual hydroxyl ions, but the higher concentration of sodium metal ion compounds reduces its solubility [20]. At the same time, the MG-W 5% is also found as the highest WPG among the MG-W wood samples.

Table 5. The Analysis Results of Impregnated Jabon Wood Physical Properties

Treatment	Density (g/cm^3)	WPG (%)	BE (%)	WU (%)	ASE (%)
Untreated	0.32±0.01^{a}	0.00±0.00^{a}	0.00±0.00^{a}	139.05±8.75^{a}	0.00±0.00^{a}
MG-S 1%	0.33±0.01^{b}	7.43±0.52^{c}	3.27±0.94^{c}	105.79±2.71^{cd}	56.02±9.23^{c}
MG-S 2.5%	0.33±0.01^{b}	8.78±0.63^{d}	3.68±1.09^{c}	95.41±2.39^{d}	61.29±3.92^{c}
MG-S 5%	0.33±0.01^{b}	7.60±0.49^{c}	3.44±0.26^{c}	103.85±9.55^{cd}	58.85±6.69^{c}
MG-W 1%	0.33±0.01^{b}	5.92±0.31^{b}	1.61±0.38^{b}	120.74±8.13^{b}	42.95±8.32^{b}
MG-W 2.5%	0.33±0.01^{b}	7.56±0.30^{c}	2.10±0.63^{b}	116.57±7.69^{bc}	48.03±8.13^{b}
MG-W 5%	0.33±0.01^{b}	7.86±0.67^{c}	3.33±1.08^{c}	106.61±0.67^{c}	57.29±4.59^{c}

$^{a-d}$ values: shows significance based on the Duncan's test
MG-S: magnetite synthesized using NaOH precursor
MG-W: magnetite synthesized using NH_4OH precursor

The treatment also led to an enhancement in luminal cell swelling caused by the large amount of polymers fulfilling the wood cavities, indicated by the increasing bulking effect (BE) [8]. Wood's shrinkage activity is avoided by the inclusion of Fe_3O_4-NP in cell wall polymers, which can restrict the water molecules' motion and improve its anti-swelling efficiency (ASE) [16], [47]. However, this is also supported by the water absorption behavior which is not like WPG and BE trends, considering the water absorption (WA) of both kinds of impregnated wood shows a downward value. The Fe_3O_4-NP layer complicates the tortuous lane of water molecules penetrating the wood [48], hence the dimensions of jabon wood are more stable and further decay can be prevented [49]. The colour of jabon wood was also darkened by this process, as depicted in Figure 7. The addition of Fe_3O_4-NP concentration to the wood samples, either in the MG-S and MG-W wood, can darken the wood colour more than that of the untreated wood used as the colour standard.

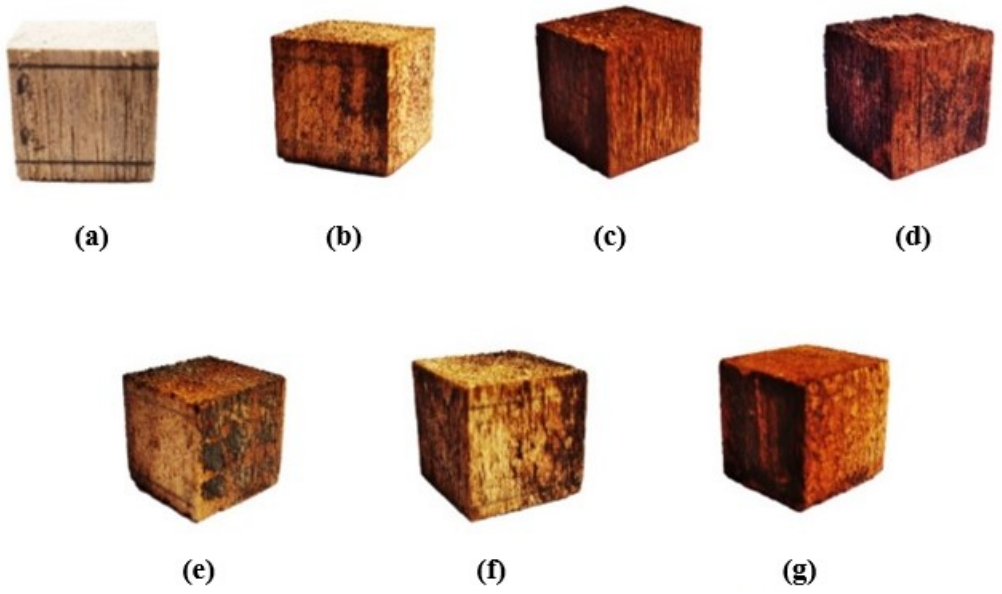

Figure 7. The Colour Change of Impregnated Jabon Wood:
(a) Untreated
(b) MG-S 1%
(c) MG-S 2.5%
(d) MG-S 5%
(e) MG-W 1%
(f) MG-W 2.5%
(g) MG-W 5%

Nevertheless, the study revealed an interesting fact, namely that the addition of different concentrations of Fe_3O_4-NP could only improve the wood density by the same value in all treatments. This contradicts the statement of Fadia et al. [50] who found that wood density increased after adding Fe_3O_4-NP concentrations. This suggests that excess Fe_3O_4-NP accumulates in specific regions of the wood, leading to clogging the wood cavities through the aspirated bordered pits, and hindering the compression of impregnated jabon wood. This could be expected, as the jabon wood's pore diameter of 130-220 µm [14]. Despite this, the most effective treatment for improving the physical features of jabon wood as determined by the previous description and statistical analyses is MG-S 2.5% and MG-W 5% wood, respectively.

5. Conclusions

Based on XRD diffractogram and FTIR spectra, Fe_3O_4-NP was successfully synthesized by the co-precipitation method with yields of 93.08% for the MG-S and 82.98% for the MG-W. The particle size of Fe_3O_4-NP as measured by the crystal size approach through XRD diffractogram analysis was 34.54 nm for the MG-S and 39.24 nm for the MG-W. The improvement of the parameters of physical properties has occurred after the impregnation process according to the hypothesis, including the wood density, WPG, BE, and ASE. Contrarily, WA experienced a decrease in value. According to Duncan's test results, the best treatment achieved by MG-S 2.5% and MG-W 5%.

References

[1] A. Rana, K. Yadav, and S. Jagadevan, "A comprehensive review on green synthesis of nature-inspired metal nanoparticles: Mechanism, application and toxicity," *J. Clean. Prod.*, vol. 272, no. 5, p. 122880, 2020.
[2] W. Bi *et al.*, "Effects of chemical modification and nanotechnology on wood properties," *Nanotechnol. Rev.*, vol. 10, pp. 978–1008, Aug. 2021.
[3] E. Garskaite *et al.*, "The Accessibility of the Cell Wall in Scots Pine (Pinus sylvestris L.) Sapwood to Colloidal Fe3O4Nanoparticles," *ACS Omega*, vol. 6, no. 33, pp. 21719–21729,

2021.

[4] V. Sharma *et al.*, "Interactions between silver nanoparticles and other metal nanoparticles under environmentally relevant conditions: A review," *Sci. Total Environ.*, vol. 653, no. 18, pp. 1042–1051, 2019, doi: 10.1016/j.scitotenv.2018.10.411.

[5] I. Kong, S. Hj, M. Hj, D. Hui, A. Nazlim, and D. Puryanti, "Magnetic and microwave absorbing properties of magnetite – thermoplastic natural rubber nanocomposites," *J. Magn. Magn. Mater.*, vol. 322, no. 21, pp. 3401–3409, 2010.

[6] J. Jayaprakash, N. Srinivasan, and P. Chandrasekaran, "Surface modifications of CuO nanoparticles using Ethylene diamine tetra acetic acid as a capping agent by sol–gel routine," *Spectrochim. Acta Part A Mol. Biomol. Spectrosc.*, vol. 123, pp. 363–368, Apr. 2014.

[7] I. Wahyuningtyas, I. S. Rahayu, A. Maddu, and E. Prihatini, "Magnetic properties of wood treated with nano-magnetite and furfuryl alcohol impregnation," *BioResources*, vol. 17, no. 4, pp. 6496–6510, 2022.

[8] G. D. Laksono, I. S. Rahayu, L. Karlinasari, W. Darmawan, and E. Prihatini, "Characteristics of magnetic sengon wood impregnated with nano fe3o4 and furfuryl alcohol," *J. Korean Wood Sci. Technol.*, vol. 51, no. 1, pp. 1–13, 2023.

[9] I. Rahayu, W. Darmawan, N. Nugroho, D. Nandika, and R. Marchal, "Demarcation point between juvenile and mature wood in sengon (Falcataria moluccana) and jabon (Antocephalus cadamba)," *J. Trop. For. Sci.*, vol. 26, no. 3, pp. 331–339, 2014.

[10] I. S. Rahayu *et al.*, "The Effect of Synthetic and Commercial Nano-Magnetite on the Electromagnetic Absorbance Behavior of Magnetic Wood," *J. Sylva Lestari*, vol. 12, no. 2, pp. 366–384, 2024.

[11] K. D. V. Nguyen and K. D. N. Vo, "Magnetite nanoparticles-TiO2 nanoparticles-graphene oxide nanocomposite: Synthesis, characterization and photocatalytic degradation for Rhodamine-B dye," *AIMS Mater. Sci.*, vol. 7, no. 3, pp. 288–301, 2020.

[12] H. Pereira, J. Graça, and J. Rodrigues, "Wood Chemistry in Relation to Quality," *Cheminform*, vol. 35, Nov. 2004.

[13] H. Krisnawati, M. Kallio, and M. Kanninen, *Anthocephalus cadamba Miq.: ekologi, silvikultur dan produktivitas*. 2011.

[14] A. Martawijaya, S. Hadjodarsono, and M. Haji, *Atlas kayu Indonesia jilid II*. Bogor (ID): Pusat Penelitian dan Pengembangan Hutan dan Konservasi Alam, 2005.

[15] A. Widiyanto and M. Siarudin, "Karakteristik Sifat Fisik Kayu Jabon(anthocephalus Cadamba Miq) Pada Arah Longitudinal Dan Radial," 2017. [Online]. Available: https://api.semanticscholar.org/CorpusID:134346950. [Accessed: Jan, 2024].

[16] C. A. S. Hill, *Wood modification: Chemical, thermal, and other processes*. West Sussex (UK): John Willey and Sons Ltd., 2006.

[17] R. Gieré, "Magnetite in the Human Body: Biogenic vs. Anthropogenic," *Proc. Natl. Acad. Sci.*, vol. 113, p. 201613349, Oct. 2016.

[18] British Standard, "Standard Methods of Testing Small Clear Specimens of Timber," 1957

[19] W. S. Peternele *et al.*, "Experimental investigation of the coprecipitation method: An approach to obtain magnetite and maghemite nanoparticles with improved properties," *J. Nanomater.*, vol. 2014, 2014.

[20] W. M. Daoush, "Co-Precipitation and Magnetic Properties of Magnetite Nanoparticles for Potential Biomedical Applications," *J. Nanomedicine Res.*, 2017.

[21] V. Dubey and V. Kain, "Synthesis of magnetite by coprecipitation and sintering and its characterization," *Mater. Manuf. Process.*, vol. 33, no. 8, pp. 835–839, Jun. 2018.

[22] A. G. Magdalena, I. M. B. Silva, R. F. C. Marques, A. R. F. Pipi, P. N. Lisboa-Filho, and M. Jafelicci, "EDTA-functionalized Fe3O4 nanoparticles," *J. Phys. Chem. Solids*, vol. 113, pp. 5–10, 2018.

[23] D. B. Fumis, M. L. D. C. Silveira, C. Gaglieri, L. T. Ferreira, R. F. C. Marques, and A. G. Magdalena, "The Effect of EDTA Functionalization on Fe3O4 Thermal Behavior," *Mater. Res.*, vol. 25, 2022.

[24] M. Wang, N. Wang, H. Tang, M. Cao, Y. She, and L. Zhu, "Surface modification of nano-Fe 3O 4 with EDTA and its use in H 2O 2 activation for removing organic pollutants," *Catal. Sci. Technol.*, vol. 2, no. 1, pp. 187–194, 2012.

[25] G. Fink, "Encyclopedia of the Elements. Technical Data, History, Processing, Applications,"

Angew. Chemie Int. Ed., vol. 44, pp. 3174–3175, 2005.

[26] J. S. J. Hargreaves, "Some considerations related to the use of the Scherrer equation in powder X-ray diffraction as applied to heterogeneous catalysts Some considerations related to the use of the Scherrer equation in powder X-ray diffraction as applied to heterogeneous catal," *Catal. Struct. React.*, vol. 2, no. 1–4, pp. 1–5, 2016.

[27] Y. Dong, Y. Yan, S. Zhang, and J. Li, "Wood/Polymer Nanocomposites Prepared by Impregnation with Furfuryl Alcohol and Nano-SiO2," *BioResources*, vol. 9, Aug. 2014.

[28] I. Khan, K. Saeed, and I. Khan, "Nanoparticles: Properties, applications and toxicities," *Arab. J. Chem.*, vol. 12, no. 7, pp. 908–931, 2019.

[29] X. Zhang, R. Zhou, W. Rao, Y. Cheng, and B. G. Ekoko, "Influence of precipitator agents NaOH and NH4OH on the preparation of Fe3O4 nano-particles synthesized by electron beam irradiation," *J. Radioanal. Nucl. Chem.*, vol. 270, no. 2, pp. 285–289, 2006.

[30] B. Y. Yu and S. Y. Kwak, "Assembly of Magnetite Nanoparticles into Spherical Mesoporous Aggregates with a 3-D Wormhole-Like Porous Structure," *Mater. Sci.*, no. 38, pp. 1–9, 2010.

[31] C. Liang *et al.*, "Superior electromagnetic interference shielding performances of epoxy composites by introducing highly aligned reduced graphene oxide films," *Compos. Part A Appl. Sci. Manuf.*, vol. 124, no. June, p. 105512, 2019.

[32] A. Altomare, N. Corriero, C. Cuocci, A. Falcicchio, A. Moliterni, and R. Rizzi, "QUALX2.0: A qualitative phase analysis software using the freely available database POW-COD," *J. Appl. Crystallogr.*, vol. 48, pp. 598–603, 2015.

[33] P. Piekarz, K. Parlinski, and A. Oleś, "Origin of the Verwey transition in magnetite: Group theory, electronic structure, and lattice dynamics study," *Phys. Rev. B*, vol. 76, Nov. 2007.

[34] J. Winsett *et al.*, "Quantitative determination of magnetite and maghemite in iron oxide nanoparticles using Mössbauer spectroscopy," *SN Appl. Sci.*, vol. 1, no. 12, p. 1636, 2019.

[35] S. Mohammed and H. Mohammed, "Characterization of Magnetite and Hematite Using Infrared Spectroscopy," *Arab J. Sci. Res. Publ.*, vol. 2, no. 1, pp. 38–44, 2018.

[36] J. Coates, "Interpretation of Infrared Spectra, A Practical Approach," in *Encyclopedia of Analytical Chemistry*, 2006.

[37] C. H. Chia, S. Zakaria, M. Yusoff, S. C. Goh, and C. Y. Haw, "Size and crystallinity-dependent magnetic properties of CoFe 2 O 4 nanocrystals," vol. 36, pp. 605–609, 2010.

[38] W. S. Chiu, S. Radiman, R. Abd-shukor, M. H. Abdullah, and P. S. Khiew, "Tunable coercivity of CoFe 2 O 4 nanoparticles via thermal annealing treatment," vol. 459, pp. 291–297, 2008.

[39] M. K. Shahid and Y. Choi, "Characterization and Application of Magnetite Particles , Synthesized by Reverse Coprecipitation Method in Open Air from Mill Scale," *J. Magn. Magn. Mater.*, p. 165823, 2019.

[40] B. X. Liang, X. Wang, J. Zhuang, Y. Chen, D. Wang, and Y. Li, "Synthesis of Nearly Monodisperse Iron Oxide and Oxyhydroxide Nanocrystals **," pp. 1805–1813, 2006.

[41] P. Zanatta, M. Lazarotto, P. Henrique, and G. De Cademartori, "The effect of titanium dioxide nanoparticles obtained by microwave-assisted hydrothermal method on the color and decay resistance of pinewood," *Maderas. Cienc. y Tecnol.*, vol. 19, no. 4, pp. 495–506, 2017.

[42] I. Ramadan, M. Moustafa, and M. Nassar, "Facile controllable synthesis of magnetite nanoparticles via a co -precipitation precipitation approach," *Egypt. J. Chem.*, vol. 65, no. 9, pp. 59–65, 2022.

[43] V. Sreeja, K. Jayaprabha, and P. A. Joy, "Water-dispersible ascorbic-acid-coated magnetite nanoparticles for contrast enhancement in MRI," *Appl. Nanosci.*, no. 5, pp. 435–441, 2015.

[44] P. B. Rathod and S. A. Waghuley, "Synthesis and UV-Vis spectroscopic study of TiO2 nanoparticles," *Int. J. Nanomanuf.*, vol. 11, no. 3–4, pp. 185–193, 2015.

[45] I. Safitri, Y. G. Wibowo, D. Rosarina, and Sudibyo, "Synthesis and characterization of magnetite (Fe3O4) nanoparticles from iron sand in Batanghari Beach," *IOP Conf. Ser. Mater. Sci. Eng.*, vol. 1011, no. 1, 2021.

[46] S. Bagheri, K. Shameli, and S. B. Abd Hamid, "Synthesis and characterization of anatase titanium dioxide nanoparticles using egg white solution via Sol-Gel method," *J. Chem.*, vol. 2013, 2013.

[47] Y. Dong, Y. Yan, Y. Zhang, S. Zhang, and J. Li, "Combined treatment for conversion of fast-growing poplar wood to magnetic wood with high dimensional stability," *Wood Sci. Technol.*, 2016.

[48] S. Holy, A. Temiz, G. Köse Demirel, M. Aslan, and M. H. Mohamad Amini, "Physical properties, thermal and fungal resistance of Scots pine wood treated with nano-clay and several metal-oxides nanoparticles," *Wood Mater. Sci. Eng.*, vol. 17, no. 3, pp. 176–185, 2022.

[49] E. Suttie, "Chemically modified solid wood . I . Resistance to fungal attack," *Mater. und Org.*, vol. 32, no. 3, pp. 159–182, 1998.

[50] S. L. Fadia, I. Rahayu, D. S. Nawawi, R. Ismail, and E. Prihatini, "The Physical and Magnetic Properties of Sengon (Falcataria moluccana) Wood Impregnated with Synthesized Magnetite Nanoparticles," *J. Sylva Lestari*, vol. 11, no. 3, pp. 408–426, 2023.